

## DESIGN AND SIMULATIONS OF PEROVSKITE-BASED SOLAR CELLS WITH EFFICIENCIES OVER 30%

Saifeldien Hesham Mohamed Aly HUSSEIN<sup>1</sup>, Andrei DRĂGULINESCU<sup>2</sup>

*Recently, numerous efforts have been directed towards improving the efficiency of perovskite-based solar cells, as a viable competitor of the ones based on silicon. In this paper, we designed and simulated five different solar cells with perovskite, with the purpose of obtaining high values of the power conversion efficiency (PCE). The highest values (36.83%, 34.19% and 33.31%) were obtained for solar cells with an active layer of p-type perovskite, n-type perovskite and a combination of perovskite and silicon, respectively. These results are higher than for the perovskite-based solar cells in literature and offer promising perspectives for future practical implementations.*

**Keywords:** solar cells, perovskite, silicon, copper indium gallium selenide (CIGS), power conversion efficiency (PCE), record efficiency, design, SCAPS-3D simulation.

### 1. Introduction

Until now, the main source of energy has been constituted by the fossil fuels – hydrocarbon-based biological materials that, when burned, provide significant amounts of energy. Every country depends on fossil fuels and this dependency has increased even more in the last 200 years. That rapid increase did not just deplete the fossil fuel reserves dramatically, but also seriously affected the climate. This situation pushed scientists and engineers towards developing renewable energy technologies, in the attempt to find sustainable and efficient alternatives to fossil fuels. Solar energy has the advantages that it never runs out and is the biggest and cheapest of all sources of energy on our planet [1].

An efficient device that uses solar energy is the solar cell. There are three major types of solar cells: monocrystalline, polycrystalline, and thin-film ones. The first two types are generally based on silicon, whereas thin-film solar cells can have, as materials for the active layer, amorphous silicon, cadmium telluride (CdTe), CIGS, gallium arsenide (GaAs), various organic materials, various dyes (in dye-sensitized solar cells) and perovskites, respectively. Moreover, solar cells

<sup>1</sup> Eng., ARRK Research & Development SRL, Cluj-Napoca, Romania, e-mail: seifhesham96@gmail.com

<sup>2</sup> Assoc. Prof., Dept. of Electronic Technology and Reliability, University POLITEHNICA of Bucharest, Romania, e-mail: andrei.dragulinescu@upb.ro; dragulinescu@yahoo.com

can also be hybrid (a combination between an organic and an inorganic material) or tandem (multiple cells connected, to increase the efficiency). The highest efficiency of a solar panel on the market is approximately 22.6% [1].

Currently, the maximum efficiency that a silicon solar cell can achieve approaches the predicted limit, leading scientists towards novel approaches. One of these is to use tandem solar cells based on perovskite and silicon, to increase efficiency without increasing the cost [2].

Perovskite materials have gone through a tremendous progress in solar cells in the last decade, probably more than any other material used in such devices. If in 2009 a research group from Tokyo, led by Tsutomu Miyasaka, developed the first perovskite solar cell (PSC), with a PCE of only 2.2%, recently a PSC with 25.2% was reported, this value being extremely close to the record one for a crystalline silicon solar cell: 26.7% [3].

Perovskite compounds can be denoted with  $ABX_3$ , where A is an ion of organic methylammonium ( $CH_3NH_3^+$ ), B is an ion of an anorganic material, generally lead or tin ( $Pb^{2+}$  or  $Sn^{2+}$ ) and X is an ion of a halogen element ( $Cl^-$ ,  $Br^-$  or  $I^-$ ). The most common combination is  $CH_3NH_3PbI_3$  (methylammonium lead iodide), also known with the abbreviation  $MAPbI_3$ . In a typical PSC, the active layer of  $MAPbI_3$  is surrounded by an HTL (hole transport layer) and an ETL (electron transport layer), the structure being completed by a top metal contact and a conductive substrate [3].

Perovskites can also be combined with other materials, in tandem solar cells. One such material with promising capabilities is CIGS. Solar cells based on CIGS as active layer have already reached a record efficiency of 23.35%, whereas the maximum value reported for a tandem perovskite/CIGS cell, 29%, already exceeded the one for silicon solar cells [4]. Another commonly used combination can be found in tandem perovskite/Si solar cells, with a record PCE of 29.8% [5] and a theoretical limit substantially higher than for silicon solar cells, of about 45%, with additional benefits from the easy monolithic integration of perovskite and silicon sub-cells [6]. All these tandem cells have the advantages of a wider spectral response (equal to the sum of the ones corresponding to the sub-cells), a higher open-circuit voltage (also equal to the sum for the sub-cells) and a short-circuit current equal to the minimum one in the sub-cells [7].

Due to the remarkable properties of these solutions, in our paper we designed and simulated several structures of solar cells based on perovskite and on the combinations of perovskite/Si and perovskite/CIGS, towards values of PCE that exceed 30%. The rest of the paper is organized as follows: section 2 includes the current state of research with some of the most recent results concerning perovskite-based solar cells; section 3 presents our simulation results, for perovskite, perovskite/Si and perovskite/CIGS solar cells, respectively; section 4 summarizes our results and compares them with the ones obtained in literature;

the paper ends with a conclusion section, where also some future work directions are highlighted.

## 2. State-of-art solar cells based on perovskite

Recently, based on  $\text{MAPbI}_3$ , PSCs with very good performance characteristics have been obtained. Rono et al. [8] simulated such a PSC, with a HTL layer of the polymer Spiro-OMeTAD and an ETL layer of indium gallium zinc oxide (IGZO). By a convenient optimization of the thickness and defect density for the  $\text{MAPbI}_3$  layer, HTL and ETL, and of the doping densities for HTL and ETL, a value of the PCE of 19.95% was obtained, higher than for other similar cells. Belarbi et al. [9] used the polymer PEDOT:PSS and  $\text{ZnO}$  for the HTL and ETL layers, respectively, with the same type of  $\text{MAPbI}_3$  absorber layer and, by SCAPS-1D simulations, obtained a PCE of 20.25% for thicknesses of 0.6  $\mu\text{m}$  and 0.2  $\mu\text{m}$  for the absorber and ETL layers, respectively, at the temperature of 300 K. Khattak et al. [3] fabricated similar PSC structures, with an  $\text{MAPbI}_3$  absorber layer and HTL of Spiro-OMeTAD, as in [8], but with an ETL of titanium oxide. As compared to the above attempts, the structures (a total of eight) were not simulated but fabricated (using the technique of spin-coating), with the best result of 14.7% for the PCE. Finally, to increase the efficiency, an enhanced structure was proposed, this time by simulations in SCAPS-1D, with CZTSe kesterite instead of Spiro-OMeTAD, and with  $\text{Cd}_{1-x}\text{Zn}_x\text{S}$  instead of  $\text{TiO}_2$ , achieving a record PCE of 27.13%.

To avoid the toxicity of lead, alternative materials to  $\text{MAPbI}_3$  were proposed, but Pb-free. Ahmad et al. [10] both simulated and fabricated PSCs with  $\text{Cs}_3\text{Sb}_2\text{I}_9$  (cesium antimony iodide), a material similar to perovskites, using as HTL and ETL the compounds  $\text{TiO}_2$  and Spiro-OMeTAD, with optimized values of the thicknesses for the absorber, HTL and ETL layers. The obtained PCE, after simulations in SCAPS-1D, was 12.54% (much lower than for  $\text{MAPbI}_3$ -based PSCs, but more environmentally friendly). The fabricated structure reached an efficiency of 1.07%. Danladi et al. [11] proposed PSCs where in the  $\text{MAPbI}_3$  material Pb is replaced by Sn (i.e., methylammonium tin iodide,  $\text{CH}_3\text{NH}_3\text{SnI}_3$ ). With  $\text{CuO}$  and  $\text{ZnO}$  as HTL and ETL, for optimum values of 0.6  $\mu\text{m}$  and 0.3  $\mu\text{m}$  for the thicknesses of the absorber and ETL layers, respectively, the simulation results in SCAPS-1D gave a maximum value for the PCE of 15.10%.

Recent research also approached tandem solar cells based on perovskite/CIGS. Nakamura et al. [12] achieved a maximum PCE of 26.2% in a perovskite/CIGS tandem cell with four-terminals. Salah et al. [4] used a modified version of the traditional perovskite sub-cell, without an ETL layer (and Spiro-OMeTAD for the HTL) in tandem with a CIGS sub-cell. The choice for the absorber included both iodine and chlorine ( $\text{MAPbI}_{3-x}\text{Cl}_x$ ). The simulations in

SCAPS-1D showed a 35.36% maximum value for the PCE of such a structure, after optimizations. Boukortt et al. [13], using other software solutions (Silvaco TCAD), simulated a two-terminal perovskite/CIGS tandem cell, with  $\text{MAPbI}_3$  as absorber layer in the PSC, and ultrathin-CIGS (u-CIGS) in the other sub-cell, obtaining a value of 20.84% for the PCE. Jošt et al. [5] proposed an improvement of a fabricated perovskite/CIGS tandem cell, with a PCE of 24.2%, to eliminate the mismatch in photocurrent between the sub-cells, showing by simulations that a PCE of 32% could be obtained after the optimization of the structure. Hedayati and Olyaei [7] simulated a four-terminal perovskite/CIGS tandem cell, with a p-n homojunction, using a model of the cell with the Newton method with partial differential equations and obtained a PCE of 30.71%.

Another tandem solar cell based on perovskite that has been recently researched is the perovskite/silicon one. Xu et al. [6] performed an optical modeling, using RT (light-ray tracing) and the TMM (transfer matrix method), of perovskite/Si tandem solar cells, with an improvement of the accuracy that is otherwise low when building such monolithic devices on textured substrates of Si. Yadav and Kumar [14] used AFORS-HET software to simulate two novel perovskite/Si tandem solar cells, with p/n-type Si as absorber and n/p-type doped  $\text{MAPbI}_3$  as emitter layer. By optimizing the thicknesses of the emitter and absorber layers, their doping densities and other parameters, values of 28.82% and 29.48% were achieved, respectively, for the two proposed structures. Xie et al. [15] used Silvaco Atlas simulator to characterize four-terminal perovskite/Si solar cells, in five different configurations, with the perovskite material of  $(\text{BA})_2(\text{MA})_{n-1}\text{Pb}_n\text{I}_{3n+1}$  (with  $n$  from 1 to 5), where MA is methylammonium and BA is butylammonium. The obtained structure proved an improved stability as compared to other hybrid perovskites, and a PCE of 30.58%. Messmer et al. [2] suited the PERC (passivated emitter and rear cell) technology for the bottom cell in a perovskite/Si tandem solar cell and, by simulations using Sentaurus TCAD, concluded that the efficiency of such devices could reach approximately 30%.

In our paper, we analyzed and simulated both single-junction and tandem solar cells based on perovskite and obtained values of the PCE comparable and even exceeding the ones given in literature.

### 3. Simulations of perovskite-based solar cells

We performed all simulations with the Solar Cell Capacitance Simulator SCAPS-1D, developed at the Department of Electronics and Information Systems (ELIS) of the University of Gent, Belgium. The standard conditions used for the simulations were: temperature 300 K, air mass AM 1.5, with an illumination of 1000  $\text{W/m}^2$  and 100% transmission.

First off, we simulated three different structures of  $\text{MAPbI}_3$ . The first one was a p-i-n structure, where the p and n layers are the HTL and ETL layers, respectively, and the i layer is an intrinsic  $\text{MAPbI}_3$  absorber layer. The second and the third simulated structures were a p-type and an n-type perovskite-based structure, respectively, where p-doped and n-doped  $\text{MAPbI}_3$  were correspondingly used for the absorber layer. In each of the three structures, the ETL layer was made of tin oxide, with a thickness of 0.02  $\mu\text{m}$  (first structure) and of 0.01  $\mu\text{m}$  (second and third structure). For the HTL we chose the polymer PCBM, with a thickness of 0.5  $\mu\text{m}$  (first and second structure) and Spiro-OMeTAD, with a thickness of 1  $\mu\text{m}$  (third structure). For the transparent conductive oxide (TCO) layer, we chose titanium oxide, with a thickness of 0.05  $\mu\text{m}$  (first structure) and zinc oxide, with a thickness of 0.01  $\mu\text{m}$  (second and third structure). Finally, for the back contact, we chose platinum (first and second structure) and gold (third structure). We also selected, conveniently, from the available literature, values for the bandgap, electron affinity, relative dielectric permittivity, effective density of states in the conduction band and valence band, respectively, the electron and hole thermal velocities, the electron and hole mobilities, the shallow uniform donor and acceptor densities. We obtained the JV characteristic curves, the quantum efficiency-wavelength, and the quantum efficiency-photon energy curves in each case. Also, for each structure, we deduced, from the JV curves, the solar cell parameters: open-circuit voltage ( $V_{oc}$ ), short-circuit current density ( $J_{sc}$ ), fill factor (FF), power conversion efficiency (PCE), voltage maximum power point (VMPP) and current density maximum power point (IMPP). All these values are given in the summative Table 1 in section 4 of our paper. In Fig. 1 we present the JV characteristics and in Fig. 2 the quantum efficiency as a function of the wavelength and of the photon energy, respectively, for the p-type perovskite structure, the one that achieved the highest value of the PCE among all our five simulated structures.

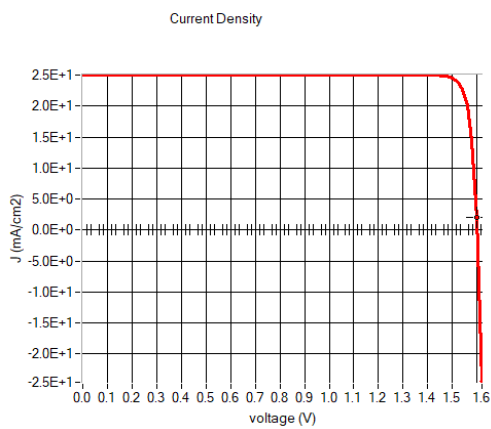


Fig. 1. JV characteristics for the structure with the highest value obtained for the PCE (p-type perovskite solar cell).

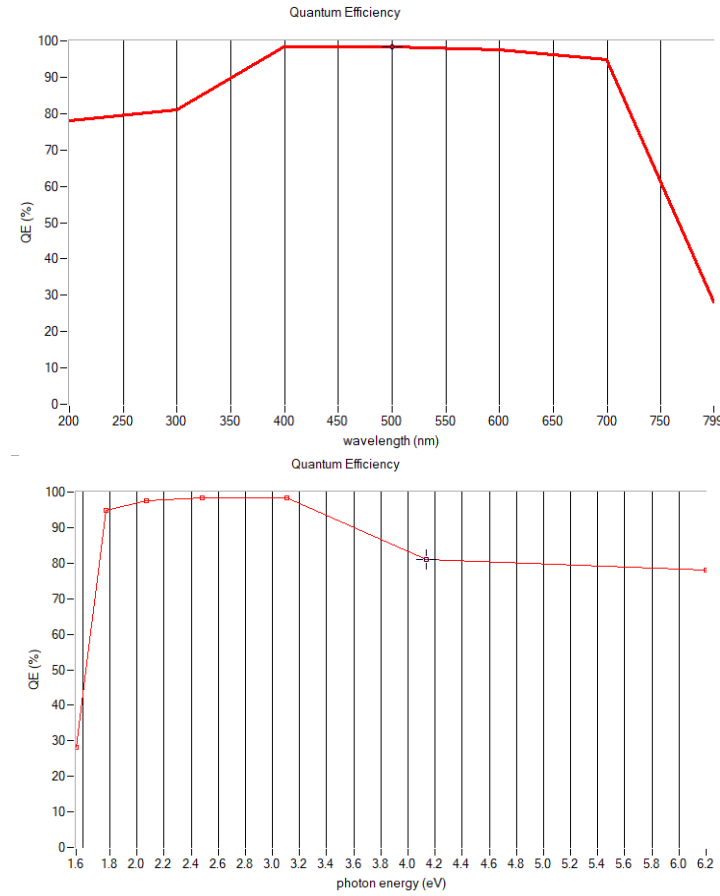


Fig. 2. Quantum efficiency – wavelength curve (up) and quantum efficiency – photon energy curve (down), for the p-type perovskite structure (the one with the highest PCE).

Secondly, we also simulated a perovskite/Si solar cell, with a structure consisting of six layers. These layers, in order from the back contact to the front of the device, with the corresponding thicknesses, are: platinum back contact, of work function 6.3; p-type silicon back surface field (p-Si BSF), 0.5  $\mu$ m; bulk layer of p-type silicon (p-Si bulk), 2  $\mu$ m; PCBM polymer as HTL, 0.5  $\mu$ m; n-doped  $\text{MAPbI}_3$ , 0.5  $\mu$ m; tin oxide as ETL, 0.01  $\mu$ m; titanium oxide as TCO layer, 0.01  $\mu$ m. The effect of heavy doping of the active layers was simulated by setting the value of doping to the optimum value suiting the compatibility of the layers and allowing the software iterations to proceed with no convergence failures.

The third type of solar cell that we simulated was a perovskite/CIGS one, with the following layers: platinum back contact, of work function 6.3; p-type CIGS, as HTL, 4  $\mu$ m; n-doped  $\text{MAPbI}_3$ , 1  $\mu$ m; tin oxide, as ETL, 0.01  $\mu$ m; zinc oxide as TCO layer, 0.01  $\mu$ m. All the results for the solar cell parameters of the

two tandem cells (perovskite/Si and perovskite/CIGS) are also given in the summative Table 1 in section 4 of our paper.

#### 4. Summary of results and comparison with other solar cells

We summed up the results obtained from our simulations of the five different perovskite-based solar cells in Table 1, together with recent results obtained in literature, for comparative purposes.

*Table 1*  
**Summary of the results obtained for the performance parameters of the five simulated solar cells, compared with recent results from literature**

Absorber layer	V <sub>oc</sub> (V)	J <sub>sc</sub> (mA/cm <sup>2</sup> )	FF (%)	PCE (%)	VMPP (V)	IMPP (mA/cm <sup>2</sup> )
Perovskite (p-i-n)	1.24	25.63	84.86	27.00	1.10	24.59
Perovskite (p-)	1.60	25.03	91.82	36.83	1.50	24.61
Perovskite (n-)	1.60	23.63	90.38	34.19	1.47	23.22
Perovskite/Si	1.54	23.83	90.83	33.31	1.43	23.31
Perovskite/CIGS	0.89	32.90	86.94	25.55	0.80	31.83
Perovskite [8]	5.32	25.55	14.68	19.95	N/A	N/A
Perovskite [9]	0.84	25.60	94.68	20.25	N/A	N/A
Perovskite [3]	1.12	26.45	88.90	27.13	N/A	N/A
Lead-free perovskite [11]	0.83	29.71	61.23	15.10	N/A	N/A
ETL-free perovskite (top cell) [4]	1.23	28.00	80.71	27.74	N/A	N/A
Perovskite/CIGS [7]	2.25	25.80	73.02	30.71	N/A	N/A

From Table 1 we can see that our five proposed structures perform well and, sometimes, even better than the ones given in recent literature, in terms of the main four performance parameters of solar cells. Because only a few references gave the values for all four parameters, some of them calculating only the final result for the PCE, in Table 2 we included a more detailed comparison, including all the cited references where the value of the PCE was calculated.

From Table 2 we can observe that, for our first simulated structure, the value of the PCE (27%) is close to other similar solar cells proposed in literature (only slightly surpassed by two structures, with 27.13% and 27.74%, respectively, and significantly higher than other two proposals, with 19.95% and 20.25%). Our next two structures, n-type and p-type doped, showed excellent values of the PCE, up to 36.83%. The fourth structure, a tandem perovskite/Si solar cell, had a PCE higher than the other two recent similar structures in literature (33.31%, as compared to 29.48% and 30.58%). Finally, the perovskite/CIGS structure, with a

PCE of 25.55%, is still higher than another recent proposal (20.84%), but can be further improved to increase even more the efficiency by means of a careful design.

Table 2

**Comparison between the values of the PCE obtained with our five structures and the ones given in recent literature. Our results are the highlighted ones. The characteristics for the solar cells proposed in literature are given in section 2.**

Absorber layer	PCE (%)	Absorber layers (tandem)	PCE (%)
<b>MAPbI<sub>3</sub></b>	<b>27.00</b>	<b>Perovskite/Si</b>	<b>33.31</b>
<b>n-doped MAPbI<sub>3</sub></b>	<b>34.19</b>	Perovskite/Si [14]	29.48
<b>p-doped MAPbI<sub>3</sub></b>	<b>36.83</b>	Perovskite/Si [15]	30.58
MAPbI <sub>3</sub> [8]	19.95	<b>Perovskite/CIGS</b>	<b>25.55</b>
MAPbI <sub>3</sub> [9]	20.25	Perovskite/CIGS [13]	20.84
MAPbI <sub>3</sub> [3]	27.13	Perovskite/CIGS [12]	26.2
MAPbI <sub>3-x</sub> Cl <sub>x</sub> and no ETL [4]	27.74	Perovskite/CIGS [7]	30.71
Cs <sub>3</sub> Sb <sub>2</sub> I <sub>9</sub> [10]	12.54	Perovskite/CIGS [5]	32
MASnI <sub>3</sub> [11]	15.10	Perovskite/CIGS [4]	35.36

## 5. Conclusions

To conclude, five different perovskite-based solar cell structures were successfully designed and simulated, after material selection, to achieve the compatibility of layers, calculating the optimum thickness of each layer, and applying heavy doping values on active layers.

The basic structure of the intrinsic perovskite-based solar cell (Perovskite p-i-n structure) achieved 27% power conversion efficiency, which is higher than the latest values in literature, whereas by modifying the intrinsic layer, to obtain two different structures of p-type perovskite and n-type perovskite layer, respectively, yielded PCE values of approximately 36.8% and 34.2%, respectively, which is significantly higher than using a pure perovskite layer, thus showing the critical effect of heavy doping.

The six layered-structure of the perovskite-silicon solar cell achieved approximately 33.3% PCE, whereas the perovskite-CIGS solar cell achieved a PCE of 25.55%.

All five structures achieved efficiencies higher than the highest value for commercialized solar cells, 22.6%. The results obtained in this paper presented a comparison between possible structures of perovskite-based solar cells and showed the effect of heavy doping on the PCE. The five proposed perovskite solar cell technologies have promising results that make them good competitors of the commercialized solar cells and of the other fabricated or simulated solar cells in literature.

Future work needs to be performed by scientists to synthesize these structures and test them. Perovskite proved to be an important class of materials for the photovoltaics industry, and it clearly deserves more focus on research. However, the challenge lies in using suitable doping techniques to achieve the proposed values. That could be a transition point in the photovoltaics industry and a big step towards commercializing perovskite-based solar panels.

## R E F E R E N C E S

- [1] *S. H. M. A. Hussein*, Design and Simulation of Solar Cells with Different Materials, Dissertation Thesis, Energy Engineering Master, Faculty of Engineering in Foreign Languages, Politehnica University of Bucharest, 2021.
- [2] *C. Messmer, J. Schön, S. Lohmüller, J. Greulich, C. Luderer, J. C. Goldschmidt, M. Bivour, S. W. Glunz and M. Hermle*, “How to make PERC suitable for perovskite–silicon tandem solar cells: A simulation study”, in *Prog. Photovolt. Res. Appl.*, **vol. 30**, no. 2, Jan. 2022, pp. 1023–1037.
- [3] *Y. H. Khattak, E. Vega, F. Baig and B. M. Soucase*, “Performance investigation of experimentally fabricated lead iodide perovskite solar cell via numerical analysis”, in *Materials Research Bulletin*, **vol. 151**, July 2022, pp. 111802.
- [4] *M. M. Salah, A. Zekry, A. Shaker, M. Abouelatta, M. Mousa and A. Saeed*, “Investigation of Electron Transport Material-Free Perovskite/CIGS Tandem Solar Cell”, in *Energies*, **vol. 15**, no. 17, Aug. 2022, pp. 6326.
- [5] *M. Jošt, E. Köhnen, A. Al-Ashouri, T. Bertram, Š. Tomšič, A. Magomedov, E. Kasparavicius, T. Kodalle, B. Lipovšek, V. Getautis, R. Schlatmann, C. A. Kaufmann, S. Albrecht and M. Topič*, “Perovskite/CIGS Tandem Solar Cells: From Certified 24.2% toward 30% and Beyond”, in *ACS Energy Lett.*, **vol. 7**, no. 4, March 2022, pp. 1298–1307.
- [6] *L. Xu, J. Liu, K. McIntosh, M. Abbott, E. Aydin, T. Allen, M. De Bastiani, M. Babics, J. Kang, M. Alamer, W. Yan, W. Liu, F. Xu, A. U. Rehman and S. De Wolf*, “Accurate Optical Modeling of Monolithic Perovskite/Silicon Tandem Solar Cells and Modules on Textured Silicon Substrates”, in *PRX ENERGY*, **vol. 1**, Aug. 2022, pp. 023005.
- [7] *M. Hedayati and S. Olyaei*, “High-Efficiency p-n Homojunction Perovskite and CIGS Tandem Solar Cell”, in *Crystals*, **vol. 12**, no. 5, May 2022, pp. 703.
- [8] *N. Rono, A. E. Merad, J. K. Kibet, B. S. Martincigh and V. O. Nyamori*, “Simulation of the photovoltaic performance of a perovskite solar cell based on methylammonium lead iodide”, in *Optical and Quantum Electronics*, vol. 54, no. 5, May 2022, pp. 317.
- [9] *M. Belarbi, O. Zeggai and S. Louhibi-Fasla*, “Numerical study of Methylammonium Lead Iodide Perovskite solar cells using SCAPS-1D simulation program”, in *Materials Today Proceedings*, **vol. 51**, no. 7, Jan. 2022, pp. 2115–2119.
- [10] *K. Ahmad, M. Q. Khan and H. Kim*, “Simulation and fabrication of all-inorganic antimony halide perovskite-like material based Pb-free perovskite solar cells”, in *Optical Materials*, **vol. 128**, June 2022, pp. 112374.
- [11] *E. Danladi, A. O. Salawu, M. O. Abdulmalik, E. D. Onoja, E. E. Onwoke and D. S. Adepehin*, “Optimization of Absorber and ETM Layer Thickness for Enhanced Tin based Perovskite Solar Cell Performance using SCAPS-1D Software”, in *PHYSICSAccess*, **vol. 2**, no. 1, March 2022, pp. 001.
- [12] *M. Nakamura, C. C. Lin, C. Nishiyama, K. Tada, T. Bessho and H. Segawa*, “Semi-transparent Perovskite Solar Cells for Four-Terminal Perovskite/CIGS Tandem Solar Cells”, in *ACS Appl. Energy Mater.*, vol. 5, no. 7, July 2022, pp. 8103–8111.

- [13] *N. E. I. Boukortt, S. Patanè, A. M. AlAmri, D. AlAjmi, K. Bulayyan and N. AlMutairi*, “Numerical Investigation of Perovskite and u-CIGS Based Tandem Solar Cells Using Silvaco TCAD Simulation”, in Silicon, July 2022.
- [14] *C. Yadav and S. Kumar*, “Numerical simulation of novel designed perovskite/silicon heterojunction solar cell”, in Optical Materials, **vol. 123**, Jan. 2022, pp. 111847.
- [15] *X. Xie, Q. Bai, G. Liu, P. Dong, D. Liu, Y. Ni, C. Liu, H. Xi, W. Zhu and D. Chen*, “Device simulation of quasi two-dimensional perovskite/silicon tandem solar cells towards 30%-efficiency”, in Chinese Physics B, **vol. 31**, March 2022, pp. 108801.